



ELSEVIER

Contents lists available at ScienceDirect

# Nuclear Instruments and Methods in Physics Research A

journal homepage: [www.elsevier.com/locate/nima](http://www.elsevier.com/locate/nima)

## Pumped helium system for cooling positron and electron traps to 1.2 K<sup>☆</sup>

J. Wrubel<sup>a</sup>, G. Gabrielse<sup>a,\*</sup>, W.S. Kolthammer<sup>a</sup>, P. Laroche<sup>a</sup>, R. McConnell<sup>a</sup>, P. Richerme<sup>a</sup>, D. Grzonka<sup>b</sup>, W. Oelert<sup>b</sup>, T. Sefzick<sup>b</sup>, M. Zielinski<sup>b</sup>, J.S. Borbely<sup>c</sup>, M.C. George<sup>c</sup>, E.A. Hessels<sup>c</sup>, C.H. Storry<sup>c</sup>, M. Weel<sup>c</sup>, A. Müllers<sup>d</sup>, J. Walz<sup>d</sup>, A. Speck<sup>e</sup>

<sup>a</sup> Department of Physics, Harvard University, Cambridge, MA 02138, United States

<sup>b</sup> IKP, Forschungszentrum Jülich GmbH, 52425 Jülich, Germany

<sup>c</sup> York University, Department of Physics and Astronomy, Toronto, Ontario, Canada M3J 1P3

<sup>d</sup> Institut für Physik, Johannes Gutenberg Universität, D-55099 Mainz, Germany

<sup>e</sup> Rowland Institute at Harvard, Harvard University, Cambridge, MA 02142, United States

### ARTICLE INFO

#### Article history:

Received 24 August 2010

Received in revised form

4 January 2011

Accepted 11 January 2011

Available online 21 January 2011

#### Keywords:

Liquid helium

Refrigerator

Penning trap

Antiproton

Antihydrogen

### ABSTRACT

Extremely precise tests of fundamental particle symmetries should be possible via laser spectroscopy of trapped antihydrogen ( $\bar{\text{H}}$ ) atoms.  $\bar{\text{H}}$  atoms that can be trapped must have an energy in temperature units that is below 0.5 K—the energy depth of the deepest magnetic traps that can currently be constructed with high currents and superconducting technology. The number of atoms in a Boltzmann distribution with energies lower than this trap depth depends sharply upon the temperature of the thermal distribution. For example, ten times more atoms with energies low enough to be trapped are in a thermal distribution at a temperature of 1.2 K than for a temperature of 4.2 K. To date,  $\bar{\text{H}}$  atoms have only been produced within traps whose electrode temperature is 4.2 K or higher. A lower temperature apparatus is desirable if usable numbers of atoms that can be trapped are to eventually be produced. This report is about the pumped helium apparatus that cooled the trap electrodes of an  $\bar{\text{H}}$  apparatus to 1.2 K for the first time. Significant apparatus challenges include the need to cool a 0.8 m stack of 37 trap electrodes separated by only a mm from the substantial mass of a 4.2 K Ioffe trap and the substantial mass of a 4.2 K solenoid. Access to the interior of the cold electrodes must be maintained for antiprotons, positrons, electrons and lasers.

© 2011 Elsevier B.V. All rights reserved.

### 1. Introduction

A long term goal of antihydrogen studies is to trap antihydrogen atoms for precise laser or microwave spectroscopy that will probe for any tiny differences between hydrogen and antihydrogen atoms [1]. A neutral atom trap offers the most efficient use of what will always be a limited number of antimatter atoms. A significant challenge is that only atoms with an energy less than about  $k_B$  (0.5 K) can be trapped in the deepest magnetic traps that can be built to confine antihydrogen atoms. The plasmas of positrons and electrons that have been used for antihydrogen production so far were produced within traps with electrodes at 4.2 K [2,3] and higher [4]. Presumably antiprotons that cool by collisions with these plasmas reach a similar temperature or can be made to do so, though methods to directly measure the temperatures of electrons, positrons and antiprotons are still being developed. (Cooling via resonant couplings to cold circuits

is not practical for the number of particles, electrodes, and electrode potentials that must be used.)

The number of  $\bar{\text{H}}$  atoms with an energy less than a 0.5 K trap depth increases sharply as the temperature of a  $\bar{\text{H}}$  atom distribution is reduced. Relevant to this work is that about ten times more  $\bar{\text{H}}$  atoms could be trapped from a 1.2 K thermal distribution than from a 4.2 K distribution. A necessary condition for producing lower temperature atom distributions are antiprotons and positrons with lower energies, and this in turn will typically require lower temperature trap electrodes as a necessary (but not sufficient) condition.

Trap electrodes colder than 4.2 K have been produced previously only for small electron traps with dimensions on the order of 1 cm. The first realization utilized a dilution refrigerator to cool cylindrical trap electrodes to below 100 mK. Quantum transitions between the lowest cyclotron states of a single suspended electron were observed and used to establish that the electron cyclotron motion came into thermal equilibrium with the 100 mK trap electrodes [5], and then later to measure the electron magnetic moment to three parts in  $10^{13}$  [6,7]. A later attempt to adapt these methods to trapping an electron in a planar Penning trap for quantum information studies realized a similar electrode temperature [8].

<sup>☆</sup> Work by the ATRAP Collaboration.

\* Corresponding author. Tel.: +1 617 495 4381.

E-mail address: [gabrielse@physics.harvard.edu](mailto:gabrielse@physics.harvard.edu) (G. Gabrielse).

Cooling trap electrodes within an antihydrogen apparatus is much more challenging than cooling a small electron trap. An  $\bar{H}$  apparatus also presents challenges that are not generally present for more familiar pumped helium configurations [9–11]. First, the ATRAP Penning trap electrodes to be cooled are a 0.8 m long stack of 37 gold-plated copper ring electrodes separated by MACOR insulators (Fig. 1). The thermal paths to these electrodes are thus through long electrical leads and through insulating spacers. Second, the electrodes to be cooled to 1.2 K are located within a 4.2 K superconducting solenoid at one end, and extend 0.4 m into the bore of a 4.2 K superconducting Ioffe trap at the other (Fig. 1), both of which must be anchored at 4.2 K to allow up to 90 A of current to flow within a centimeter of the electrodes. Third, no magnetic materials that would distort the fields of the Penning or Ioffe traps can be used. Fourth, access to the cold electrodes for antiprotons, positrons, electrons and lasers must be maintained. Fifth, uninterrupted operation over many months must be possible since the apparatus must function reliably during the six months per year that CERN provides scheduled daily shifts of antiprotons. Sixth, it is desirable that the system is

compatible with a later upgrade to a pumped  $^3\text{He}$  or a dilution refrigerator system if this becomes necessary.

The low temperature apparatus is described in Section 2. The cool-down and operation of the refrigeration system is described in Section 3, along with two different modes of operation. The design and characterization of the cooling power (Section 4), the heat load (Section 5) and the helium conductance rate (Section 6) are discussed, as is the method for coupling the electrodes to the refrigeration system (Section 7). Since this type of refrigeration system has not previously been used for particle trapping and  $\bar{H}$  studies, the basic low temperature physics and parameters needed to design such a system are summarized.

To illustrate the potential usefulness of the apparatus and methods reported here, we append in Section 8 a brief demonstration of the possibility to form low temperature plasmas of electrons and positrons within the 1.2 K system. By measuring the oscillation frequency of the center-of-mass of a plasma suspended within a Penning trap, and also the frequency of an internal oscillation mode of the trapped plasma, we can deduce the density and shape of the trapped single-component plasma [12]. Shifts in these frequencies indicate changes in plasma temperature [13]. For a spherical plasma we observe that increasing the 1.2 K temperature of the electrodes by 3 K increases the measured plasma temperature by the same amount.

Finally, the possibility of attaining lower temperature electrodes is evaluated in light of what has been learned, in Section 9.

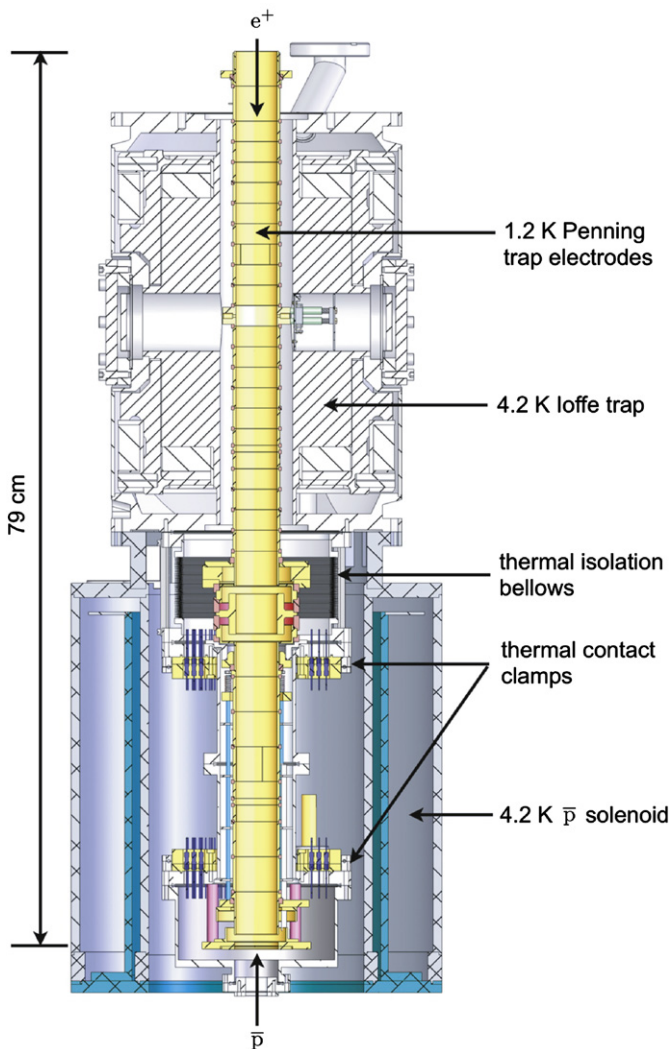


**Fig. 1.** Cylindrical ring electrodes are cooled to 1.2 K while surrounded and mechanically supported by a 4.2 K Ioffe trap apparatus from above, and surrounded by a 4.2 K solenoid. Within a vertically directed 1 T bias field from an external solenoid (not shown), the 1.2 K electrodes are biased to form Penning traps for  $\bar{p}$ ,  $e^+$  and  $e^-$ . A refrigerator-cooled shield (not shown) encloses this apparatus.

## 2. The 1.2 K apparatus

The principal components of the modular 1.2 K system (Fig. 2) are made of nonmagnetic materials. OFE copper is used where this is mechanically possible to improve the thermal conductivity.

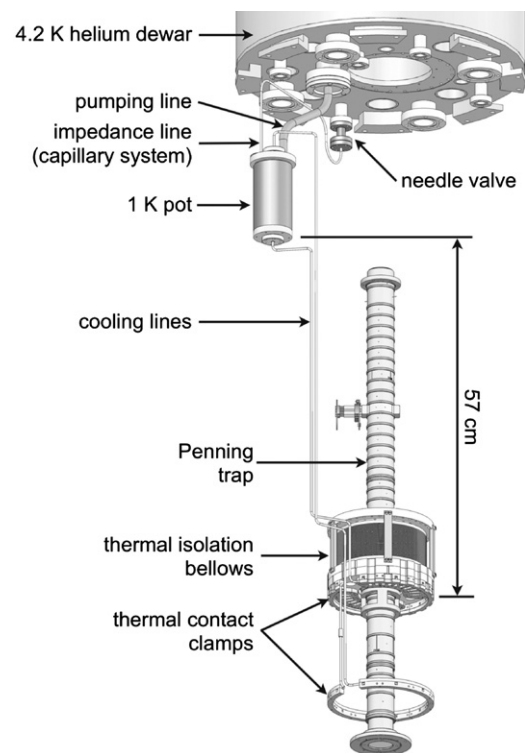


**Fig. 2.** Essential components of the 1 K refrigeration system that cools the Penning trap electrodes. Helium from a 4.2 K dewar goes through a capillary system to the 1 K pot reservoir which is pumped to make the helium into a superfluid. The superfluid He flows down to cool thermal clamps to the vacuum enclosure (not shown) that supports the trap electrodes to be cooled to 1.2 K.

Modular vacuum connections are made using 34 mm diameter, mini conflat flanges made of commercially pure grade 2 titanium. Superleak tight joints between titanium and copper are made by hydrogen brazing 99.95% silver adapters to OFE copper and electron beam welding the silver adapter to a titanium conflat flange.

Liquid helium from a large 4.2 K reservoir is filtered through a 5  $\mu\text{m}$  pure silver filter paper (Sterlitech) to prevent the entry of particle impurities that could clog the capillaries that follow. The filtered helium goes through a home built needle valve that can be adjusted by turning a G-10 tube that extends outside the cryogenic system. The titanium needle has 1.4 threads/mm (36 threads/in.) and a 7° taper to allow fine adjustments of the helium impedance and flow. The silver valve body is welded between two titanium conflat flanges using an electron beam. The design requirement to use only nonmagnetic materials led to an unusual design for the needle valve, such that it is a good thermal short along its length. Usually these valves are made of a soft metal such as brass with a stainless steel needle and flanges. To avoid magnetic field distortions nominally nonmagnetic ferrous alloys are not used. Instead, titanium is used for the needle and flanges. Since this could not be easily joined to brass we made the valve seat from pure silver that was electron-beam welded into titanium mini conflat flanges.

The helium next flows through a 3  $\mu\text{m}$  silver filter and into a capillary system embedded in a 3.2 mm ( $\frac{1}{8}$  in.) diameter titanium tube with a 0.4 mm (0.016 in.) wall thickness that takes the helium to a small reservoir, called the 1 K pot or simply the pot (Fig. 2). The helium passes through the impedance of the capillary system at 4.2 K and cools to 1.1 K by the time it reaches the 1 K pot. The thermal conductance of the impedance is small to minimize the heat flow from the 4.2 K reservoir to the pot. To minimize the chance of a complete blockage, four parallel polycarbonate capillaries (Paradigm Optics) are epoxied (with Stycast 2850 FT epoxy) within the titanium tube. Each has a 60  $\mu\text{m}$  inner diameter and has 10 of its 20 cm length epoxied inside the tube.

The final ten centimeters of the four capillaries extend through a top flange into the 221  $\text{cm}^3$  volume of the 1 K pot. This titanium 1 K pot (56 mm and 109 mm inner diameter and length) is electron-beam welded to titanium end flanges with three mini conflat flanges on the top and one on the bottom. The pot is pumped through the top flange by an external scroll pump (BOC Edwards GVSP30). A 2 mm ID orifice that is 0.25 mm (0.010 in.) thick reduces film flow into the line. The pumping lowers the temperature of the helium to 1.1 K, well below the lambda point of helium so that it is a superfluid. The inside of the 1 K pot is partly filled with an OFE copper cylinder (56 mm ID x 51 mm ID x 102 mm), which reduces the temperature gradients in the helium during pump down of the 1 K pot.

The superfluid helium fills a gold-plated, annealed OFE copper cooling line that carries the liquid through the bottom flange of the 1 K pot to the titanium vacuum enclosure that houses the trap electrodes, and back through the third top flange into the 1 K pot. In steady state, the superfluid helium fills this 290 cm long tube in intimate contact with the walls of the tube. This cooling line has a 3.2 mm ( $\frac{1}{8}$  in.) outer diameter and a 0.5 mm (0.020 in.) wall with ends brazed into silver plugs and electron-beam welded to titanium conflat flanges. Two turns of the cooling lines are clamped between gold-plated OFE copper plates. These plates are anchored with screws to titanium flanges that support the Penning trap, and through which pass the electrical leads for the trap electrodes. Gold-plating was used to ensure good thermal conduction between the clamped parts.

The vacuum enclosure for the trap includes a titanium bellows whose thermal conductivity is low enough to isolate the 1.2 and 4.2 K sections of the apparatus. The Mewasa edge-welded bellows

has 37 convolutions of 0.1 mm thick titanium and is capped with titanium conflat flanges. This bellows is rigidly fixed against compression under vacuum by five 6.4 mm x 12 mm x 85 mm G10 support posts with their fibers aligned along the length of the post to minimize thermal contraction in that direction.

The conductance of the pumping line from the pot to room temperature is sufficient to allow neglecting any pressure drop over this distance. The titanium pumping line is partially isolated from the 1 K pot by the 2 mm diameter orifice mentioned above. The line extends upward 229 mm with a 19 mm (0.75 in.) outer diameter and a 0.90 mm (0.035 in.) wall thickness titanium tube to where it is anchored to the 4.2 K liquid helium reservoir. At this point the tube expands to a 35 mm (1.375 in.) inner diameter that continues to room temperature.

Baffling within the 4.2 K upper section of the pumping line eliminates the heat load on the 1 K pot from room temperature radiation through the line, so the pot sees only 4.2 K radiation. A 29 mm (1.125 in.) OFE copper tube inside the pumping line has 4 thin copper plates spaced at 76 mm intervals, with each plate blocking more than half of alternating sides of the tube. The bottom inner surface of the copper tube is blackened with carbon black supplied by Aquadag, as is the bottom of the plates.

The 1.10 K base temperature of the pot was measured with a ruthenium oxide sensor (Lakeshore RX-202A-C) calibrated between 0.1 and 40 K. That sensor was in turn used to calibrate a Cernox sensor (CX-1030-CU), also mounted on the pot, from 40 to 1.10 K in a 1 T bias field, although neither sensor is greatly affected by the field. The standard 3-parameter function recommended for Cernox sensors from 300 to 4.2 K

$$\log_{10}(T) = c_0 + \frac{c_1}{\log_{10}(T)} + \frac{c_2}{\log_{10}(T)^2} \quad (1)$$

fits very poorly at lower temperatures. However, our calibration data fits well to a four-parameter function,

$$\log_{10}(T) = \frac{c_0}{T^{c_3}} + \frac{c_1}{\log_{10}(T)} + \frac{c_2}{\log_{10}(T)^2} \quad (2)$$

with an exponent  $c_3 \approx 1.2$ . Between 300 and 4.2 K the fit tracked the usual Cernox function to  $\pm 5\%$  of the temperature. Below 4.2 K, the fit was within an excellent  $\pm 10$  mK of the temperature sensor calibration.

### 3. Cool-down and operation

#### 3.1. Cool-down

Rapid cooling of the trap electrodes is difficult because the electrodes must be nearly thermally isolated if they are to eventually be maintained at 1.2 K. Fig. 3 shows the temperatures of the 1 K pot and the trap electrodes as the apparatus is cooled. Also on this figure is the temperature of a surrounding, refrigerator-cooled radiation shield of the “insert dewar” that surrounds the trap apparatus.

Before cool-down the needle valve is opened at least one turn. This minimizes the possibility that the valve becomes stuck during cooling, as a result of the silver seat having a larger thermal contraction coefficient than the titanium needle. The pumping line is then evacuated using a scroll pump and refilled with helium gas three times to flush out residual nitrogen gas. Helium gas at 1.5 atm is left in the pumping line.

While the surrounding dewar is being cooled by its refrigerator, liquid nitrogen is used to cool the large helium reservoir, Ioffe trap, and solenoid. About 100 mTorr of dry nitrogen or neon exchange gas in the surrounding dewar vacuum space improves the coupling of the helium dewar and the trap electrodes and

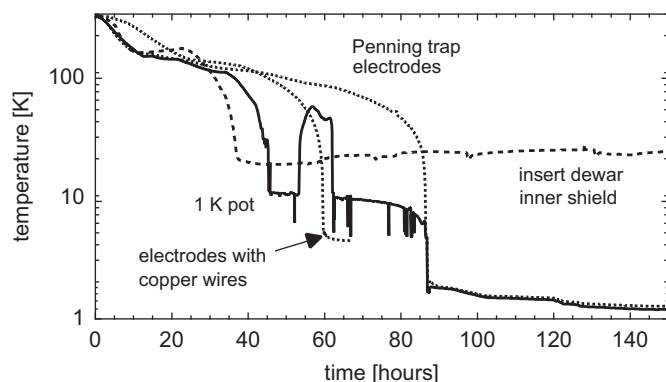


**Fig. 3.** Cool down of the 1 K pot (solid), the many Penning trap electrodes (dotted), and the pulse-tube cooled innermost radiation shield (dashed) that encloses them. Once liquid fills the cooling lines, there is no longer a significant temperature difference between the 1 K pot and electrodes.

speeds the initial cool down. The first 10 h represented in Fig. 3 shows the rapid cooling of the pot and electrodes to 120 K. The exchange gas is removed after 30 h while the temperature is high enough so that it does not cryopump to cold surfaces.

A transfer of liquid helium into the helium reservoir starts at 34 h in Fig. 3, and the temperature of the pot begins to drop. When liquid helium begins to accumulate in the helium reservoir at 42 h the pot temperature drops in 3.5 h to 11 K. The pot cools primarily by convection of the helium gas in the pumping line. This is demonstrated at 53 h when the helium gas is evacuated from the pumping line and pot and the pot temperature rises rapidly. At 62 h the pot is repressurized to 1.5 atm of helium, and the pot temperature drops.

The electrodes are poorly coupled to the pot when no liquid helium is in the copper tubes that later carry helium between the pot and the vacuum enclosure for the electrodes. (For a later cool down, two 4.8 mm ( $\frac{3}{16}$  in.) diameter copper wires added between the pot and electrode container speed the cooling by about 26 h as illustrated by the dotted curve in Fig. 3.) The electrodes continue to cool slowly over the next 40 h. Once liquid helium starts to collect in the pot, and hence enters the cooling lines, the electrode temperature drops more rapidly. At 86 h in Fig. 3, liquid helium starts to collect in the pot and cooling lines and both temperatures drop very rapidly to 4.2 K.

About 20 min later the helium pressurization line is closed off, and a butterfly valve on the scroll pump opened over a few minutes. In 15 min the temperature is at 1.8 K. The needle valve is then closed so that any superfluid helium in the pumping line is pumped away. After 24 h the temperature is 1.46 K, and the needle valve is opened one eighth of a turn. With a steady state level of helium established within the 1 K pot, the temperature decreases steadily. It then takes several days for the electrodes to reach their 1.2 K base temperature.

### 3.2. Continuous flow operation

The consumption of liquid helium during continuous flow operation is about 10 cm<sup>3</sup>/h. Adding in all other heat loads on the 4.2 K helium dewar due to the 1 K system components results in an additional 36 cm<sup>3</sup>/h of helium loss. This would drain the 40 L dewar in 870 h, which is much less than the evaporation of helium due to other components.

During continuous flow operation, the needle valve is used to adjust the flow of liquid into the pot, so that the minimum temperature is obtained, and the minimum amount of liquid helium is consumed. The adjustment is quite sensitive. Opening

the needle valve just one half turn makes its impedance negligible compared to that of the capillaries.

An increase in the temperature and pressure of the pot, along with increased gas flow through the pump, indicate that too much helium is entering the pot. The completely filled pot is overflowing the pumping orifice, and superfluid helium is in the pumping line. This helium couples efficiently to the 4.2 K helium dewar. The heat load on the pot increases, raising the pot's temperature, its pressure and the gas flow from the pot as well.

Recovery is straightforward but not always quick. The needle valve is closed all the way until the temperature, pressure, and flow return to normal. This can take up to half a day. Normal operation is restarted by opening the needle valve an eighth of a turn.

If the temperature of the pot rises while the pressure and helium gas flow fall, then the pot is running dry. The needle valve is then opened an additional one eighth of a turn.

In practice, the needle valve rarely needs to be adjusted once the optimal setting is found. Unattended operation for weeks is routine.

### 3.3. One-shot operation

The 1 K system can be operated in a one-shot mode in which no helium enters the 1 K pot through the needle valve and capillary system. This can be done by deliberately closing the needle valve. If the impedance lines become blocked, as can happen after months of continuous operation, then an involuntary one-shot operation is the only way to continue low temperature operation.

Consider first the case that the 221 cm<sup>3</sup> volume of the pot and the 11 cm<sup>3</sup> volume of the copper cooling lines are completely filled through the impedance of the capillaries before the needle valve is shut. One-shot operation at 1.2 K is then possible for the 23 h it takes to use up the helium in the pot at the measured consumption rate.

If the pot cannot be filled through the impedance due to blockage, then operation at 1.2 K can continue by liquifying helium gas to fill the pot. The pumping line is typically pressurized to about 1.5 atm to condense helium on the 4.2 K surface of the pumping line. After 30–45 min the monitored gas flow into the pumping line decreases. This indicates that the pot is full along with much of the pumping line section that is at 4.2 K.

With the pressurized helium gas closed off, the butterfly valve on the scroll pump is slowly opened over a few minutes to lower the temperature of the liquid. The pot regains its base temperature in about 20 min. Roughly half of the helium in the pot boils off to lower the temperature of the helium from 4.2 to 1.2 K. However, since much of this helium was in the pumping line outside of the 1 K pot, we recover the situation above and find a 1.2 K hold time of about 24 h.

How much helium gas is required for one liquification cycle? To condense 500 mL of liquid helium requires about 380 L of He gas at STP. A single 9.1 m<sup>3</sup> cylinder of helium can thus be used to fill the 1 K pot about 24 times.

## 4. Cooling power

The cooling of a pumped <sup>4</sup>He system is dominated by the latent heat of evaporation of He atoms across the liquid–gas interface in the 1 K pot. The cooling power of the pumped helium system is essentially determined by the number of atoms per second that are removed by the room temperature pump. The gas flow exiting the pump was measured by water displacement during continuous flow operation to be 125 cm<sup>3</sup>/min = 5.1 × 10<sup>19</sup> atoms/s. The latent



heat of evaporation at 1.1 K is 82 J/mol [14], so that the cooling power is 6.9 mW at 1.15 K. The available power to cool the apparatus is actually only about 3.4 mW (point in Fig. 4) because about 50% of the power (42 J/mol) is needed to cool the 4.2 K helium to 1.1 K. This available cooling power in steady state is equal to the heat load on the system.

The base temperature depends upon the heat load. A simple estimate of the relationship can be made using the differentiated ideal gas law,

$$\dot{Q} = P\dot{V} = \dot{N}k_B T \quad (3)$$

where  $k_B$  is Boltzmann's constant. The pumping speed  $\dot{V}$  is that of the pump through the pumping line. The predicted curve in Fig. 4 uses the expected pumping speed versus pressure of the Edwards GVSP30 scroll pump (running on 230 V at 50 Hz power). At the measured pressure of 55 Pa, this pumping speed is  $\dot{V} = 19 \text{ m}^3/\text{h}$ .

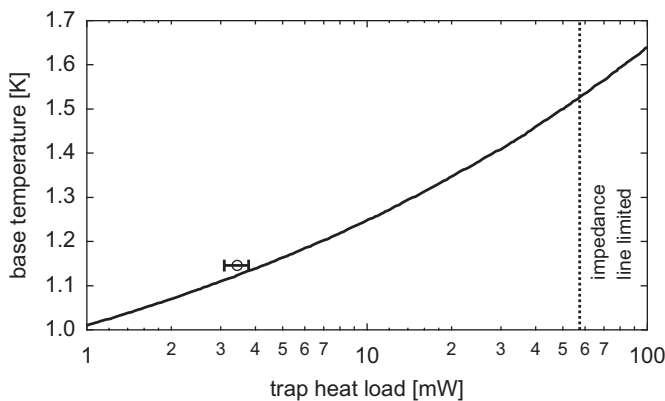


**Fig. 4.** The predicted (solid line) and measured (circle) base temperature versus the total heat load on the 1 K system (not including the power required to cool the 4.2 K liquid helium to 1.1 K). The vertical dots show the limit imposed by the maximum possible helium flow through the impedance line.

**Table 1**  
Integrated thermal conductivities [11,15],  $\bar{\lambda}$ , for materials used in the 1 K system.

Material	$\bar{\lambda}$ (300–4.2 K) (mW/cm K)	$\bar{\lambda}$ (4.2–1.1 K) (mW/cm K)
Constantan (in dc wires)	180	4
OFE copper	1600	50
G10	3.8	0.6 @ 4.2 K
MACOR	16	0.3
PTFE (teflon in coax)	20	
Stainless steel (in coax)	103	2
Titanium (CP grade 2)	118	5.4

**Table 2**  
Heat loads on the 1.2 K system.

Component	Area (cm <sup>2</sup> )	Length (cm)	$\Delta T$ (K)	$\dot{Q}$ (mW)	Quantity	Total $\dot{Q}$ (mW)
Pumping line	2.84	23	3.1	0.67	1	0.7
Isolation bellows (Ti)	0.42	61	3.1	0.11	1	0.1
Bellows spacers (G10)	0.76	8.5	3.1	0.16	5	0.8
Coax cables (copper)	0.00032	167	3.1	0.0003	40	0.01
Coax cables (teflon)	0.0031	167	3.1	0.001	40	0.05
Coax cables (stainless)	0.013	100	3.1	0.001	2	0.00
Coax cables (teflon)	0.018	100	3.1	0.011	2	0.02
Constantan (DC lines)	$4.6 \times 10^{-5}$	200	295	0.012	150	1.8
Gas cooling of pumping line						-0.7
Superfluid creep						0.5
Total estimate						3.3
Measured						3.4

The estimate assumes that the conductance of the pumping line is large enough that the pumping speed at the pot is nearly that of the scroll pump. This is demonstrated with the pot temperature measured to be 1.15 K. The pressure is measured with a thermocouple gauge (calibrated with He gas) to be 55 Pa at the location where the gas reaches room temperature. This pressure corresponds to a <sup>4</sup>He boiling point of 1.13 K. The good agreement demonstrates the negligible pressure drop along the pumping line.

The measured heat load at our measured base temperature (point in Fig. 4) agrees very well with the prediction (solid curve in Fig. 4). The predicted base temperature increases with heat load up to the cooling power limit set by the maximum helium flow through the capillaries (dotted line in Fig. 4). Above this limit, the temperature should rise more rapidly than the predicted curve due to insufficient cooling power.

## 5. Heat loads and thermal conductance

The radiation load on the 1.2 K system from 4.2 K or 20 K surroundings is negligible. The four 4.2 K baffles in the pumping line, discussed above, reflect and absorb the 300 K heat radiated down the pumping line.

Most of the heat load on the 1.2 K system is from thermal conduction. The power transferred through a sample of cross-section  $A$  that has a temperature difference  $\Delta T$  across its length  $l$  is given by

$$\dot{Q} = \bar{\lambda} \frac{A}{l} \Delta T. \quad (4)$$

Average thermal conductivities  $\bar{\lambda}$  of relevant materials are in Table 1. The most important heat loads are summarized in Table 2.

The largest conduction heat load is from the many 76  $\mu\text{m}$  (0.003 in.) diameter Constantan wires that supply dc potentials to the electrodes, since these are not heat sunk. The heat load through the coax cables is less because they are heat sunk at both 77 and 4 K. The rest of the conduction heat load is from the thermal isolation bellows and the pumping line, both of which connect to 4 K. However, we assume that gas cooling of the pumping line by the escaping helium gas is large enough to eliminate this conduction heat load.

Superfluid film creep up the pumping line contributes an extra heat load. The creep is mitigated by the 2 mm diameter orifice in the 1 K pot before the pumping line, and is proportional to the circumference of the constriction [11,16]. For clean glass this is  $7 \times 10^{-5} \text{ S cm}^2/\text{s}$ , where  $S$  is the circumference of the orifice, but this flow is thought to be ten times higher for metals due to

microscopic surface roughness [11]. Therefore, a rough estimate for the superfluid flow up the pumping line is  $1.6 \text{ cm}^3/\text{h}$ . Although only a portion of this helium flow is recondensed on the 1 K pot and thereby contributes to the heat load, we take a worst case estimate in which all of the helium flow recondenses, and therefore adds 0.5 mW to the heat load.

The electrodes are separated from each other by electrically and thermally insulating MACOR spacers. Under equilibrium conditions there is no heat load directly on the electrodes, so no temperature gradients are expected due to the MACOR, but they will increase the time-constant for cooling the stack. A rough estimate suggests that the 1/e time constant for cooling from 4.2 to 1.1 K is 24 s, and this is negligible compared to other times in the system.

The agreement between the estimated and measured heat loads is extremely good, somewhat better than could be expected given the approximations.

## 6. Helium flow conductance

In continuous flow mode, an equilibrium gas flow of  $\dot{N} = 5.1 \times 10^{19}$  atoms/s from the 1 K pot (discussed in Section 4) is currently needed. Half of the cooling power associated with this flow is required to cool the incoming helium from 4.2 to 1.15 K. The other half is needed to compensate the 3.4 mW residual heat load on the 1 K system. Our system is designed so that this helium flow is determined by the fixed pumping speed of the pump and by the adjustable impedance of the needle valve, with plenty of excess cooling power available in case a later apparatus modification makes it necessary to deal with a higher heat load. It should be noted that there may be some cooling contributed by Joule–Thomson expansion of the helium in the thermally insulated capillaries.

### 6.1. Pumping line

The connection of the 1 K pot to the vacuum pump is designed to have a conductance large enough that the pumping speed at the pot is very nearly the pumping speed of the vacuum pump. The pumping line starts with the narrow orifice that limits superfluid film creep out of the 1 K pot (Section 5). The helium gas flow through this orifice is viscous flow, as is all flow through the pumping line. The calculation of the viscous and possibly turbulent flow through an orifice is more complicated than needed to design an adequate pumping line. Instead we use the simpler formula for molecular flow through an orifice of area  $A$ ,

$$\dot{N} = \frac{\dot{V}P}{kT} = 2.61 \times 10^{24} \frac{PA}{\sqrt{TM}} \quad (5)$$

since this generally gives a lower limit on viscous flow through the same geometry. The flow rate is in atoms/s when the pressure,  $P$  is in Pascal, the area is in  $\text{m}^2$ , the temperature  $T$  is in Kelvins, and  $M$  is the mass number [11]. For  $^4\text{He}$  with a 2 mm orifice,  $\dot{N} = 2.15 \times 10^{20}$  atoms/s of gaseous He at 1.1 K and 55 Pa. Since this is about four times the measured helium flow of  $5.1 \times 10^{19}$  atoms/s, the orifice is sufficiently large. Our assumption here has been that all of the pumping speed is due to gaseous flow through the orifice, but as discussed in Section 5, the superfluid film will also contribute positively to the effective pumping speed.

The gaseous flow between the orifice and the pump is described by combining Eqs. (7) and (8) and the differentiated ideal gas law Eq. (3)

$$\dot{N}_{\text{gas}} = \frac{P_{\text{avg}} \dot{V}}{k_B T_{\text{avg}}} = \frac{\pi a^4 P_{\text{avg}} \Delta P}{8 \eta l k_B T_{\text{avg}}} \quad (6)$$

**Table 3**

Flow conductance calculations for the 1.2 K system.  $P_1$  and  $P_2$  are the pressures at the entering and exiting ends of the tube, respectively.

ID (cm)	$l$ (cm)	$T_{\text{avg}}$ (K)	$\dot{N}kT_{\text{avg}}$ (Pa L/s)	$\eta$ ( $\times 10^{-6}$ Pa s)	$P_1$ (Pa)	$P_2$ (Pa)	$\Delta P$ (Pa)	
(1)	1.1	19	2.6	1.83	0.955	55.3	55.3	0.019
(2)	3.2	45	4.2	2.96	1.26	55.3	55.3	0.0014
(3)	3.5	44	150	106	12.8	55.3	55.0	0.34
(4)	3.5	40	295	208	19.7	55	54.1	0.92
(5)	6.0	174	295	208	19.7	54.1	53.6	0.47

where  $T_{\text{avg}}$  is the average temperature, and  $P_{\text{avg}}$  the average pressure between the ends of the tube.

The pumping line is modeled with a series of five tube sections (Table 3), for which the average viscosity of gaseous  $^4\text{He}$  is approximately  $\eta \approx 5.18 \times 10^{-7} T_{\text{avg}}^{0.64}$  Pa s. Most of the pressure drop is in the room temperature sections of the line. The total pressure drop between the mechanical pump and the pot with  $\dot{N} = 5.1 \times 10^{19}$  atoms/s is only 1.8 Pa, which is much smaller than the pressure of 55 Pa measured in the fourth section of the pumping line. Therefore, the pressure differential in the pumping line is negligible.

Although helium is not so well described by the ideal law at low temperatures due to the van der Waals forces between atoms, the nonideal behavior generally increases the conductance of a given geometry [17]. This makes the approximations of this section a bit more conservative, and thus still appropriate for designing the pumping line.

### 6.2. Impedance of the capillaries

For the fixed pumping speed for helium from the pot, the helium flow (and hence the cooling power of the system) increases as the needle valve is opened. The increase continues until the impedance of the capillaries to liquid helium flow is larger than that from the needle valve. The capillaries thus determine the maximum cooling power that can be accommodated by this pumping system, as well as providing some thermal isolation between 4.2 and 1.1 K.

Four parallel  $60 \mu\text{m}$  ID capillaries, each 20 cm long, are epoxied into the 2.4 mm ID titanium tube that connects the needle valve to the pot. The number of atoms per second,  $\dot{N}$ , that flow through the capillaries is equal to the product of the fluid atomic density  $\rho$  and the volume flow,  $\dot{V}$ . Therefore, by using the impedance for viscous flow,  $Z \equiv \Delta P/\eta \dot{V}$ , we get

$$\dot{N} = \rho \dot{V} = \frac{\rho}{\eta} \frac{\Delta P}{Z}. \quad (7)$$

The viscous flow is proportional to the pressure difference across the length of the capillaries,  $\Delta P$ , and inversely proportional to the fluid viscosity,  $\eta \approx 2 \times 10^{-6}$  Pa s.

Calculating the impedance is challenging in this case where liquid turns into gas along the length of the capillary due to the pressure drop. A reasonable starting point would seem to be the Pouseille impedance for laminar flow through a capillary of radius  $a$  and length  $l$  [17],

$$Z = \frac{8l}{\pi a^4}. \quad (8)$$

Our capillary would thus have an impedance  $Z = 1.57 \times 10^{11} \text{ cm}^{-3}$  for laminar flow. This corresponds to a flow of  $\dot{N} = 7 \times 10^{21}$  atoms/s, and a cooling power of 940 mW, which is much larger than we anticipate that will ever be needed.

However, the flow is more complicated than laminar viscous flow, and the resulting impedance higher than given by Eq. (8).

After the high thermal conductivity needle valve, the fluid will be a two-phase mixture of liquid and gaseous helium. The two-phase mixture enters the capillaries where the pressure drops along the length of the capillary, boiling more liquid and creating a larger fraction of gas.

Historically, the right impedance for a capillary system has been found by trial and error. A typical impedance for other 1 K systems [18,9] is in the several  $10^{11} \text{ cm}^{-3}$ , and specifically a value of  $6.7 \times 10^{11} \text{ cm}^{-3}$  was found to give a critical cooling power of 15 mW [18]. This is about four times larger than our impedance.

We opted for an adjustable needle valve to avoid time consuming adjustments of the capillary impedance. The needle valve provided enough flexibility that we were able to adjust the flow impedance for robust operation on our first trial.

## 7. Cooling the trap electrodes

One of the unique features of this apparatus is that space limitations due to the presence of the close-fitting Ioffe trap and antiproton solenoid (Fig. 1), force the 1 K pot reservoir to be far from the major heat load at the trap electrodes. The connection between the 1 K pot and the electrode stack is made with a 290 cm long, 0.22 cm ID, gold-plated OFE copper tube which extends from the pot, encircles the trap twice, and returns to the pot (Fig. 2). In such a tube at low temperatures, the thermal conductivity of the copper is negligible, and instead we rely upon the much higher thermal conductivity of the helium II liquid within the tube. In contrast, during the initial cooling of the experiment from room temperature, the conductivity of the copper is the dominant source of cooling for the electrodes.

In such an extended geometry it could be important to consider the finite thermal conductivity of the helium II in cooling the electrodes. Helium at temperatures below the lambda point of 2.17 K consists of two fluids. One is a superfluid component which increases from a fraction of the total density  $\rho_s/\rho = 0$  at 2.17 K to 0.99 at 1 K, and the other component is normal fluid such that the total density is constant  $\rho = \rho_s + \rho_n \approx 2.2 \times 10^{22} \text{ atoms/cm}^3$ . The superfluid component can be considered to have no viscosity or entropy, whereas the normal fluid component has both viscosity and entropy.

Although the effective thermal conductivity of helium II is quite high, there is no heat transport through the superfluid component itself [14]. Rather, cooling is achieved because the zero entropy superfluid component of the helium flows towards the heat load, where it becomes normal fluid with a molar entropy of  $s_\lambda = 8.2 \text{ J/mol/K}$  [19]. The extra normal fluid then flows in the opposite direction to the superfluid, carrying entropy back to the pot.

The heat load in our apparatus  $\dot{Q} = 3.4 \text{ mW}$  requires an equilibrium atomic flow rate  $\dot{N}_n = N_A \dot{Q} / T s_\lambda = 2.08 \times 10^{20} \text{ atoms/s}$ , where  $N_A$  is Avogadro's number. Using Eqs. (7) and (8), the pressure gradient required to produce such a flow is only 0.11 Pa. Then using the helium II fountain pressure equation  $\Delta T = \Delta P / \rho s$  [14], we find that no significant temperature gradient results due to this flow.

However, because of the very low density of normal fluid at 1.2 K,  $\rho_n = 5.65 \times 10^{20} \text{ atoms/cm}^3$  [19], there is a very high atomic velocity  $v_n = \dot{N}_n / 2A\rho_n = 5.03 \text{ cm/s}$ . This is much larger than both the superfluid counterflow velocity  $v_s = 0.13 \text{ cm/s}$  and the superfluid critical velocity  $v_{s,c} = 0.81 \text{ cm/s}$  [20]. The large velocity difference,  $v_r = |\vec{v}_n - \vec{v}_s|$ , results in a frictional force between the normal and superfluid components due to vortex turbulence in the superfluid. The temperature gradient due to this frictional interaction is approximately [14,21]

$$\nabla T = A(T) \frac{\rho}{s_\lambda N_A} (v_r - v_0)^2 v_r \quad (9)$$

where  $A(1.2 \text{ K}) \approx 100 \text{ cm s/mol}$ , and we will approximate  $v_0 \approx v_{s,c}$ . (The useful equations in Ref. [14] were used with corrections based upon the original references cited and a review [21].) The result for a 3.4 mW heat load is a gradient  $\nabla T = 1.7 \text{ mK/m}$ . Using an average length of the conductance tubes of 145 cm gives  $\Delta T = 2.5 \text{ mK}$ .

Other sources of temperature gradient are also expected to be small. For instance, the Kapitza resistance [11] between the helium and cooling line is only about 2.5 mK. However, at a pot temperature of 1.15 K, the Penning trap electrodes are measured to be 1.23 K, which is 80 mK warmer than the pot. The source of this gradient has not been positively identified, but we tentatively attribute this difference to gradients in the complicated geometries in the vacuum can.

## 8. Cold electrodes make cold plasmas

To demonstrate the potential usefulness of this cryogenic system, we observe the effect of changing the temperature of the trap electrodes in Fig. 1 upon the quadrupole mode resonance frequency of a 53 million electron plasma suspended at the center of one of the trap electrodes. The line shown as a function of time in Fig. 5 is the temperature of the trap electrodes measured with a calibrated Cernox sensor mounted on the stack. Twice during the 5 h shown in the figure we increased the measured electrode temperature by 3 K, from a base temperature of 1.3 K. This is done by sealing off the scroll pump and pressurizing the pot with 1.5 atm of helium gas, whereupon the electrode temperature slowly rises. Then the pressurization valve is closed, the butterfly valve to the pump valve is opened, and the electrode temperature decreases.

One physics motivation for cold electrodes is to reduce the temperature to which blackbody radiation heats plasmas of electrons and positrons suspended within the electrodes. The electrons and positrons in the strong magnetic field of the Penning trap emit synchrotron radiation to cool to the temperature set by the blackbody radiation. An important application of these cold plasmas is to make antihydrogen atoms that are cold enough to be trapped. The cold electrons can be used to cool antiprotons with which they collide. The cold positrons, when they interact with cold antiprotons, can both cool the antiprotons and form antihydrogen atoms.

Accumulation of cold electrons and cold positrons within the electrodes of a Penning trap is accomplished by applying appropriate voltages to the trap electrodes, along with a strong

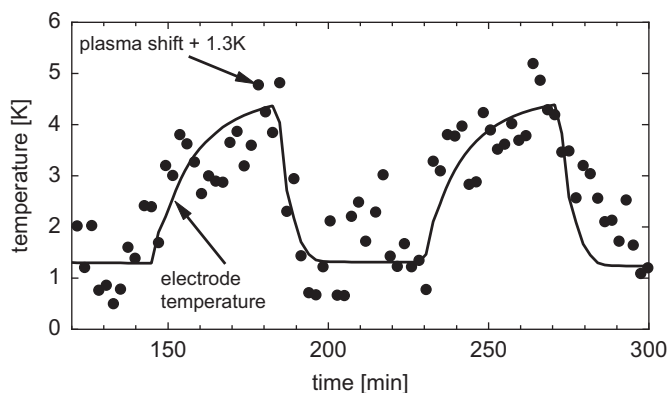


Fig. 5. Measured electrode temperature (solid curve) versus time. For a nearly spherical electron plasma of 53 million electrons, the measured plasma temperature shifts (dots), track the shifts in the electrode temperature. The unknown plasma temperature offset is adjusted to make it possible to directly compare the temperature shifts.

magnetic field (1 T) directed along the symmetry axis of the cylindrical ring electrodes. The resulting fields will suspend a cold plasma of one or the other species near the center of a trap electrode.

To deduce the temperature of a suspended positron or electron plasma, we drive the plasma with a radio frequency voltage between the electrode within which the particles reside and a neighboring electrode. With the right choice of frequency we can excite an oscillatory motion of the plasma's center-of-mass. Alternatively, at a higher frequency we can excite an internal oscillation of the positrons or electrons in which the ends of the plasma oscillate out of phase with each other, which is the quadrupole mode. Both oscillation modes induce radio frequency currents in the trap electrode that can be measured to determine the two plasma resonance frequencies.

For the spheroidal plasma shape that is the equilibrium configuration of an electron or positron plasma in an ideal Penning trap, these two oscillation frequencies and the number of particles in the plasma determine the shape and density of the spheroid [12]. For the trapped electrons in Fig. 5 the shape is very close to a sphere. For a spheroid, the shift of the quadrupole frequency squared is proportional to the temperature shift of the plasma [13].

The circles in Fig. 5 show that the plasma temperature changes by just the amount that the temperature of the electrodes changes. The temperature offset for these measurements is not determined by the plasma frequency measurements. It is chosen to be the temperature of the 1.3 K electrodes before they are warmed up. It seems very unlikely that the two temperatures would track so closely unless the plasma is in equilibrium at the temperature of the electrodes. This is consistent with a steady state plasma temperature that equals the 1.3 K trap temperature. Detailed experimental studies of the plasma temperatures are in process.

Exactly what this temperature means must be studied further in light of the expectation that the radial and axial motions become increasingly decoupled as the temperature is reduced [22], observed primarily at higher densities than employed here [23]. Large electron plasmas with temperatures approaching our electrode temperature have not previously been studied, and only a small number of positrons have been cooled via collisional couplings to laser-cooled ions surrounding them in a Penning trap [24]. The pumped helium refrigeration opens the way to careful studies of extended plasmas of electrons and positrons at much lower temperatures than previously realized.

For plasma shapes that are not close to being spherical, and for larger plasmas that extend nearer to the trap electrodes, significant computations are required to convert measured plasma frequency shifts to temperatures. Such plasmas geometries can now be studied in detail.

## 9. Possible improvements

The initial cool-down of the apparatus is quite lengthy, and decreasing this time would be a significant improvement. There are several reasons for the slow cool down. The Penning trap is necessarily well thermally isolated from the 4.2 K Ioffe trap, and when there is no liquid helium in the 1 K system, it is also well isolated from the 1 K pot. In turn, the 1 K pot is well-isolated from the 4.2 K helium reservoir to which it is attached, and only cools by the convection of helium gas in the pressurized pumping line. This leads to a situation where the slow removal of heat from the Penning trap electrodes dominates the initial cool-down time. One solution is to transfer helium into the pot through the pumping line. This would cool the 1 K pot to 4.2 K, and would

allow liquid dripping down towards the Penning trap to cool the electrodes.

Another solution is to attach a gas thermal link that conducts the heat from the Penning trap into the Ioffe trap until the link cools to a temperature that is low enough to cryopump the gas within the link and stop the conduction. Replacing the nitrogen exchange gas with neon during cool-down [25] seems simpler since the 27 K boiling point would allow neon to remain in the system during a significant portion of the cool-down with liquid helium. Unfortunately, the surrounding refrigerator-cooled shields cool much more slowly than does the trap apparatus and the neon instead conducts heat from the shields to the trap apparatus.

Another significant improvement would be the prevention or elimination of the blockage of the impedance lines which occurred after about two months of continuous operation. The blockage requires switching the mode of operation to one-shot. To remove what is probably nitrogen-ice in the lines, a heater system has been added to the 1 K pot and impedance lines. The heater system has yet to be tested for removing blockage, but it is expected to be able to remove plugs without warming up the rest of the experiment.

A longer term improvement is to add a closed cycle  $^3\text{He}$  or dilution refrigerator system, building off the major components of the 1 K pot system, to lower the temperature of the same electrodes. A charcoal pumped  $^3\text{He}$  system could achieve temperatures of 0.3 K with several milliwatts of cooling power. A dilution refrigerator could achieve temperatures below 0.1 K with 400  $\mu\text{W}$  of cooling power. The significant reduction in heat load required for operation of a dilution refrigerator is typically achieved by heat sinking to the 1 K pot. In this way the major heat loads in Table 2 are eliminated. For instance, by heat sinking the G10 and titanium in the thermal isolation bellows at their mid-point to the 1 K pot, the heat load on the trap is reduced to 10 and 40  $\mu\text{W}$ , respectively.

## 10. Conclusions

The temperature of Penning trap electrodes of a system used to produce antihydrogen atoms is reduced by coupling them to a pumped helium refrigeration system. The design goal of 1.2 K electrodes is realized and demonstrated, despite the significant challenges posed by the substantial and intricate apparatus needed for antihydrogen production. The promise of this system is demonstrated by measuring the temperature shift of an electron plasma suspended within the cold electrodes, and found to be in good agreement with the temperature shift of the electrodes.

## Acknowledgments

This work is primarily supported by the NSF and AFOSR of the US. Other support for ATRAP is from the BMBF, DFG, and DAAD of Germany, along with the NSERC, CRC, CFI and OIT of Canada. W.O. was supported in part by CERN. Thanks to I. Silvera for useful comments on the manuscript.

## References

- [1] G. Gabrielse, in: P. Bloch, P. Pavlopoulos, R. Klapisch (Eds.), *Fundamental Symmetries*, Plenum, New York, 1987, pp. 59–75.
- [2] G. Gabrielse, N.S. Bowden, P. Oxley, A. Speck, C.H. Storry, J.N. Tan, M. Wessels, D. Grzonka, W. Oelert, G. Schepers, T. Seifick, J. Walz, H. Pittner, T.W. Hänsch, E.A. Hessels, *Phys. Rev. Lett.* 89 (2002) 213401.



- [3] G. Gabrielse, N.S. Bowden, P. Oxley, A. Speck, C.H. Storry, J.N. Tan, M. Wessels, D. Grzonka, W. Oelert, G. Schepers, T. Sefzick, J. Walz, H. Pittner, T.W. Hänsch, E.A. Hessels, *Phys. Rev. Lett.* 89 (2002) 233401.
- [4] M. Amoretti, et al., *Nature* 419 (2002) 456.
- [5] S. Peil, G. Gabrielse, *Phys. Rev. Lett.* 83 (1999) 1287.
- [6] B. Odom, D. Hanneke, B. D'Urso, G. Gabrielse, *Phys. Rev. Lett.* 97 (2006) 030801.
- [7] D. Hanneke, S. Fogwell, G. Gabrielse, *Phys. Rev. Lett.* 100 (2008) 120801.
- [8] P. Bushev, S. Stahl, R. Natali, G. Marx, E. Stachowska, G. Werth, M. Hellwig, F. Schmidt-Kaler, *Eur. Phys. J. D* 50 (2008) 97, P. Bushev, S. Stahl, R. Natali, G. Marx, E. Stachowska, G. Werth, M. Hellwig, F. Schmidt-Kaler, *Eur. Phys. J. D* 57 (2010) 301.
- [9] F. Pobell, *Matter and Methods at Low Temperatures*, third ed., Springer, New York, 2007.
- [10] R.C. Richardson, E.N. Smith (Eds.), *Experimental Techniques in Condensed Matter Physics at Low Temperatures*, Key-Westview, New York, 1998.
- [11] G.K. White, P.J. Meeson, *Experimental Techniques in Low-Temperature Physics*, fourth ed., Oxford University Press, New York, 2002.
- [12] D.H.E. Dubin, *Phys. Rev. Lett.* 66 (1991) 2076.
- [13] M.D. Tinkle, R.G. Greaves, C.M. Surko, R.L. Spencer, G.W. Mason, *Phys. Rev. Lett.* 72 (1994) 352.
- [14] W.E. Keller, *Helium-3 and Helium-4*, Plenum Press, New York, 1969.
- [15] J.G. Hust, in: R.P. Reed, A.F. Clark (Eds.), *Materials at Low Temperatures*, American Society for Metals, Metals Park, OH, 1983.
- [16] E. Ambler, N. Kurti, *Philos. Mag.* 43 (1952) 1307.
- [17] G. Nunes Jr., in: R.C. Richardson, E.N. Smith (Eds.), *Experimental Techniques in Condensed Matter Physics at Low Temperatures*, Key-Westview, 1998.
- [18] L. DeLong, O. Symko, J. Wheatley, *Rev. Sci. Instr.* 42 (1971) 147.
- [19] R.J. Donnelly, C.F. Barenghi, The observed properties of liquid helium at the saturated vapor pressure, 2010 <<http://www.uoregon.edu/rjd/vapor1.htm>>.
- [20] P. Bendt, *Phys. Rev.* 127 (1962) 1441.
- [21] W.F. Vinen, in: C.J. Gorter (Ed.), *Progress in Low Temperature Physics*, vol. 3, North-Holland, Amsterdam, 1961, p. 1.
- [22] T.M. O'Neil, P.G. Hjorth, *Phys. Fluids* 28 (1985) 3241.
- [23] B.R. Beck, J. Fajans, J.H. Malmberg, *Phys. Rev. Lett.* 68 (1992) 317.
- [24] B.M. Jelenkovic, A.S. Newbury, J.J. Bollinger, W.M. Itano, T.B. Mitchell, *Phys. Rev. A* 67 (2003) 063406.
- [25] J.N. Kidder, *Rev. Sci. Instr.* 38 (1967) 555.